

Review result of “Spatiotemporal patterns of temperature inversions and impacts on surface PM_{2.5} across China” (egusphere-2025-4751)

Response to Reviewer #1:

reviewer's comments are given in blue,

our responses are given in deep red.

Some of the content in the manuscript have been revised and updated.

Major Comments

1. The authors classify Surface-Based Inversions (SBIs) as those with a base height (H_b) < 100 m and Elevated Inversions (EIs) as 100 m ≤ H_b ≤ 2000 m. While this follows some previous studies, the specific rationale for the 100 m threshold is not sufficiently justified. Given that this threshold directly influences the reported frequencies and subsequent correlation analyses with PM_{2.5}, its appropriateness across all of China's diverse terrains (e.g., plateau stations, urban areas) should be demonstrated. The authors should provide a stronger justification, supported by literature or a sensitivity analysis, showing how the results might be affected by a different, physically-based threshold (e.g., related to the nocturnal boundary layer height).

Response: We thank you for this constructive comment regarding the robustness of the SBI classification threshold.

We verify the robustness of the 100 m threshold as suggested. We initially selected the 100 m threshold based on established methodologies in previous studies (Kahl 1990; Guo et al. 2020; Huang et al. 2021), which allows for direct cross-study comparisons.

To address your concern about terrain diversity, we re-calculated the frequencies of TI, SBI, and EI using stricter (50 m) and looser (150 m) thresholds. As shown in the newly added Figures S18–S20 (also pasted below for your reference), while the absolute magnitude of frequencies shifts slightly as expected, the spatial distribution patterns and seasonal variations remain strikingly consistent across all thresholds. This confirms that the choice of 100 m does not introduce bias into the core conclusions of the paper. We have added a brief statement in Section 2.2 citing the literature and referring to these new supplementary figures to justify the robustness of our method.

Revised: (For additional validation at different thickness thresholds, please refer to supplementary Figures S18-S20.)

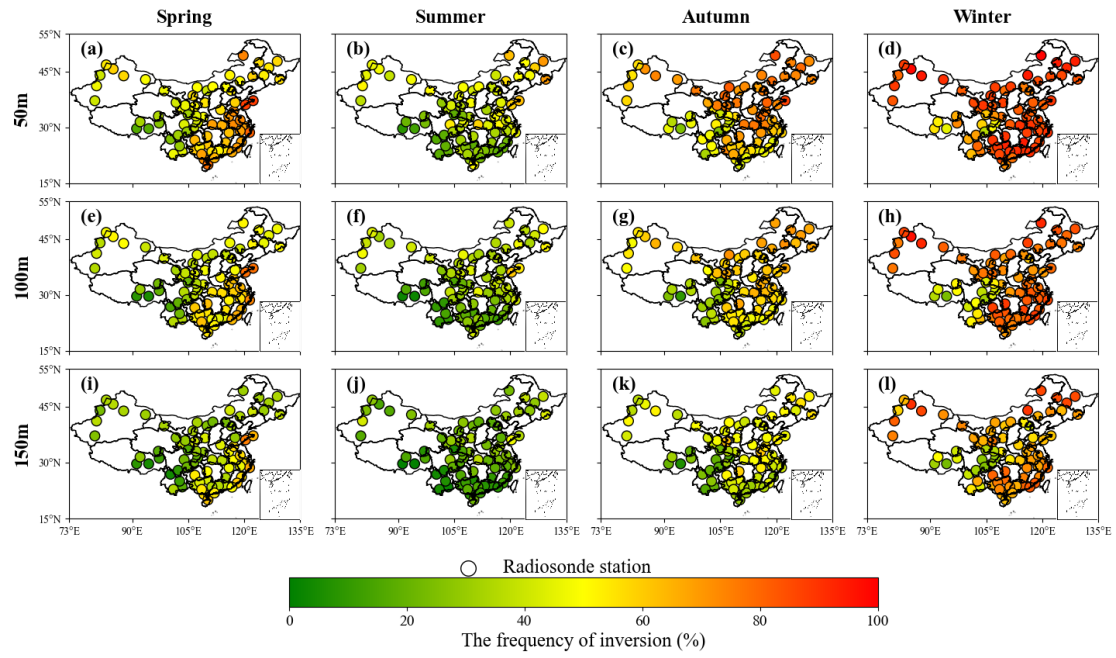


Fig. S18 Distribution of TI frequency across different thickness thresholds

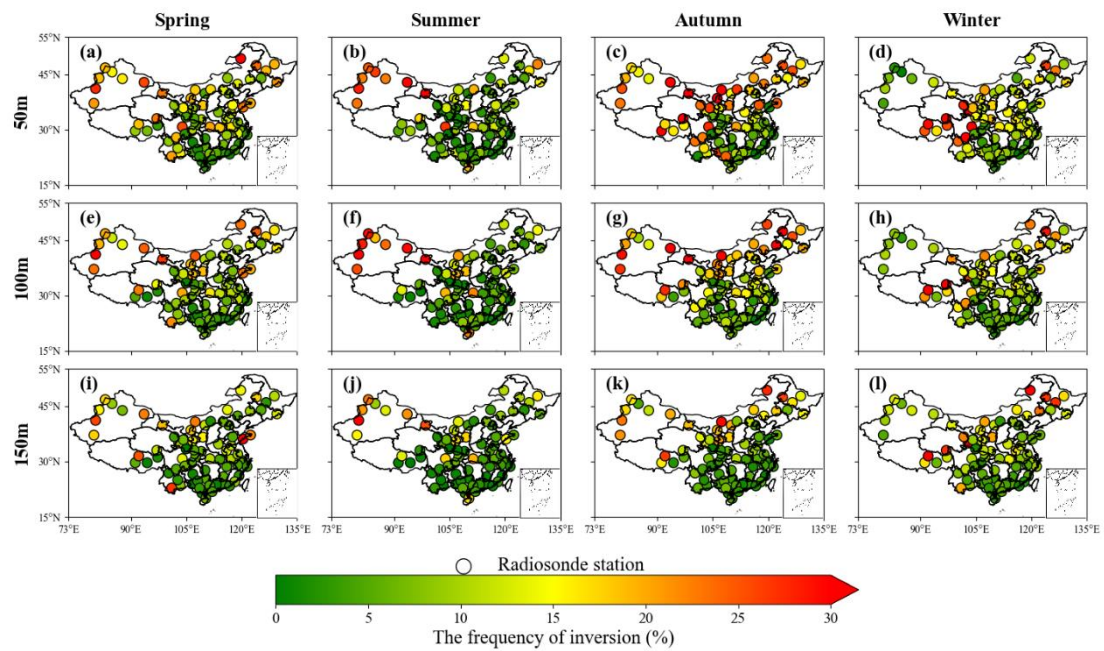


Fig. S19 Distribution of SBI frequency across different thickness thresholds

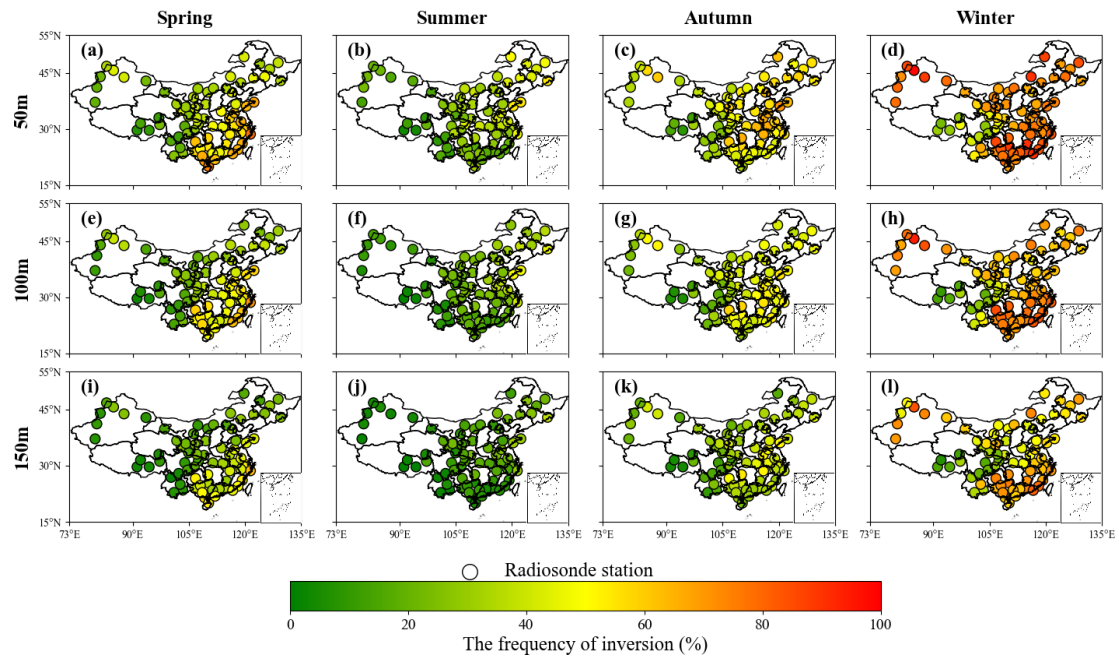


Fig. S20 Distribution of EI frequency across different thickness thresholds

2. The study effectively establishes a statistical association between TI parameters and PM concentrations. However, the assertion of a direct causal impact requires more support. The analysis does not fully disentangle the influence of emissions and synoptic-scale meteorology, which co-vary with inversion conditions. For instance, are the observed PM increases during SBIs primarily due to the inversion trapping locally emitted pollutants, or are the same large-scale stagnant conditions that cause the inversion also responsible for accumulating pollutants via regional transport? The authors should strengthen their causal interpretation by, for example, discussing the diurnal emission cycles or incorporating analysis of wind patterns and back-trajectories during specific inversion events to better attribute the pollution buildup.

Response: Thank you very much for your suggestion. To establish a stronger causal link, we have added a detailed meteorological analysis for the Beijing case study (Fig. 1), incorporating surface wind speed alongside TI strength and $\text{PM}_{2.5}$ concentrations. The causal impact of TI is clearly demonstrated through the comparison of two distinct periods: Local Trapping Period (A->B): During this stage, wind speeds remained consistently below the 2 m s^{-1} threshold (indicated by the dashed line), effectively shutting down regional transport. The progressive accumulation of $\text{PM}_{2.5}$ to peak levels synchronized with the intensification of TI strength. This confirms that under stagnant synoptic conditions, the TI-induced "lid effect" is an important factor for trapping local emissions. Dispersion Period (C->D): In contrast, when wind speeds increased significantly ($> 4 \text{ m s}^{-1}$), the enhanced horizontal ventilation and mechanical erosion of the inversion layer led to a rapid decline in $\text{PM}_{2.5}$. This "control experiment" provided by nature confirms that while low wind speeds set the stage, the presence of a strong TI is the key mechanism responsible for the actual buildup of severe

pollution.

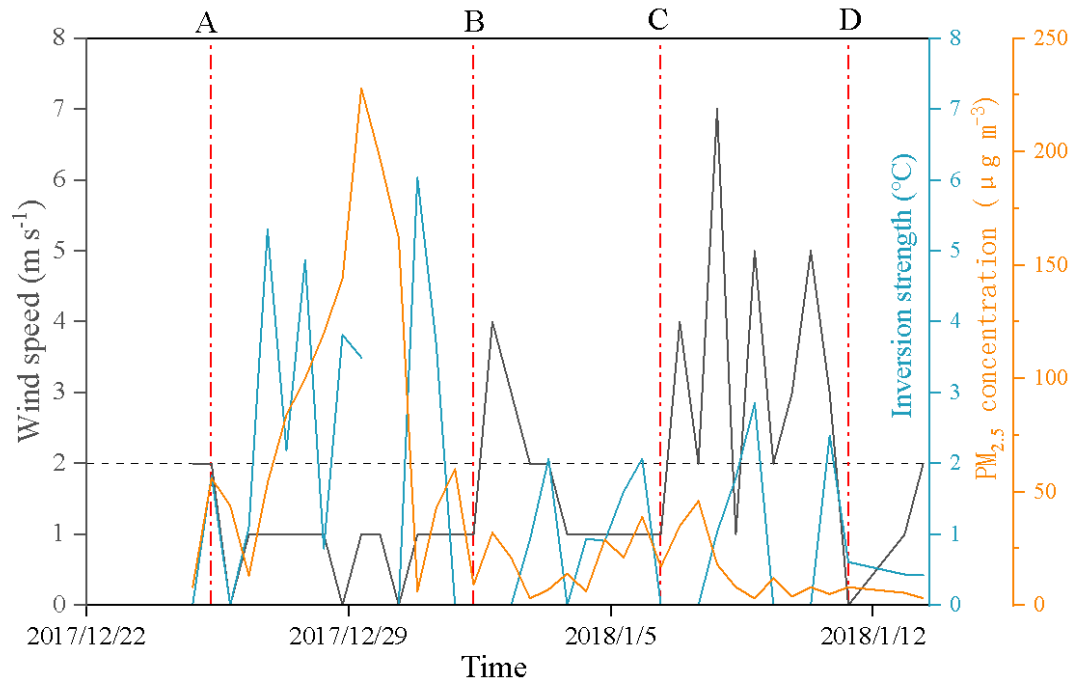


Fig. 1 Temporal evolution of surface wind speed, TI strength, and $\text{PM}_{2.5}$ concentration during a typical pollution episode in Beijing. The horizontal dashed line indicates the 2 m s^{-1} wind speed threshold. Periods A \rightarrow B and C \rightarrow D highlight the pollution accumulation under stagnant conditions and the subsequent dispersion driven by increased wind speed, respectively.

3. The division of China into seven regions is a key aspect of the analysis, but the criteria for this specific partitioning are not clearly defined. The description in Section 2.1 mentions "integrated meteorological characteristics and major urban agglomerations," but this is vague. A more explicit justification is needed. For example, why is the Sichuan Basin grouped within the larger Southwest region rather than being treated separately, given its unique meteorology? The authors should provide a clear rationale or reference an established regional framework, perhaps including a map that overlays key topographic or climatic boundaries with the regional divisions.

Response: We thank you for this critical comment regarding our regional classification.

Following your suggestion, we have clarified the rationale in the revised manuscript. We clarified that our partitioning follows the standard geographical and climatic divisions widely adopted in recent atmospheric research in China. For instance, Fan et al. (2020) and Sun et al. (2024), both of which adopted the same seven-region framework for national-scale air pollution analysis. This ensures that our results remain statistically comparable with the broader community standards. The references are included at the end of this document.

Rationale for the Southwest: We explicitly acknowledge your valid point regarding the unique

meteorology of the Sichuan Basin. While we retained the standard "Southwest" grouping to maintain consistency with the cited frameworks, we have ensured that our analysis treats the distinct mechanisms of the basin separately from the plateau areas. For instance, in Section 4.1.1, we specifically differentiate between the inversion mechanisms in the Sichuan Basin (dominated by lower-tropospheric inversions) and the Plateau (dominated by high winds and turbulence).

Revised text: We have updated the sentence in Section 2.1 to explicitly state the criteria: "To capture this diversity, we partition the domain (excluding Hong Kong, Macau, and Taiwan owing to data limitations) into seven regions based on standard administrative divisions, integrated meteorological characteristics and major urban agglomerations (Fig. 1)."

4. The authors mention that temperature inversions primarily affect PM_{2.5} pollution in winter and are one of the causes of severe pollution events. However, this viewpoint is mainly based on nationwide averages and lacks a detailed analysis of specific case studies. To enhance the persuasiveness of the conclusions, it is recommended that the authors include case studies of several major city clusters, such as the Beijing-Tianjin-Hebei region, the Yangtze River Delta, and the Pearl River Delta. These city clusters face different climatic and geographic conditions, and analyzing specific cases would provide a more comprehensive understanding of the actual impact of temperature inversions on PM_{2.5} pollution, especially during severe pollution events.

Response: We appreciate this constructive suggestion. You are correct that nationwide averages might obscure the specific dynamics of pollution events in different regions.

Following your recommendation, we selected three representative cities—Beijing (representing Beijing-Tianjin-Hebei, BTH), Nanjing (representing Yangtze River Delta, YRD), and Yangjiang (representing Pearl River Delta, PRD)—and analyzed the temporal evolution of TI strength and PM_{2.5} concentrations during specific heavy pollution episodes (added as Fig.S22 in the revised manuscript).

The case study analysis reveals distinct regional characteristics: In Beijing (Fig. S22a) and Nanjing (Fig. S22b), we observed a clear accumulation process. TI intensification serves as the trigger, followed by a progressive rise in PM_{2.5}. The pollution often persists due to high emission loads even when TI fluctuates, demonstrating the "lid effect." In Yangjiang (Fig. S22c), the PM_{2.5} concentrations show a tighter, near-synchronous correlation with TI strength. This suggests that in the PRD region, where background pollution is lower, air quality is highly sensitive to immediate changes in vertical stability.

These case studies provide robust evidence supporting our conclusion that temperature inversions are a primary driver of pollution accumulation, while also highlighting the role of emission loads in modulating the lag time of this relationship.

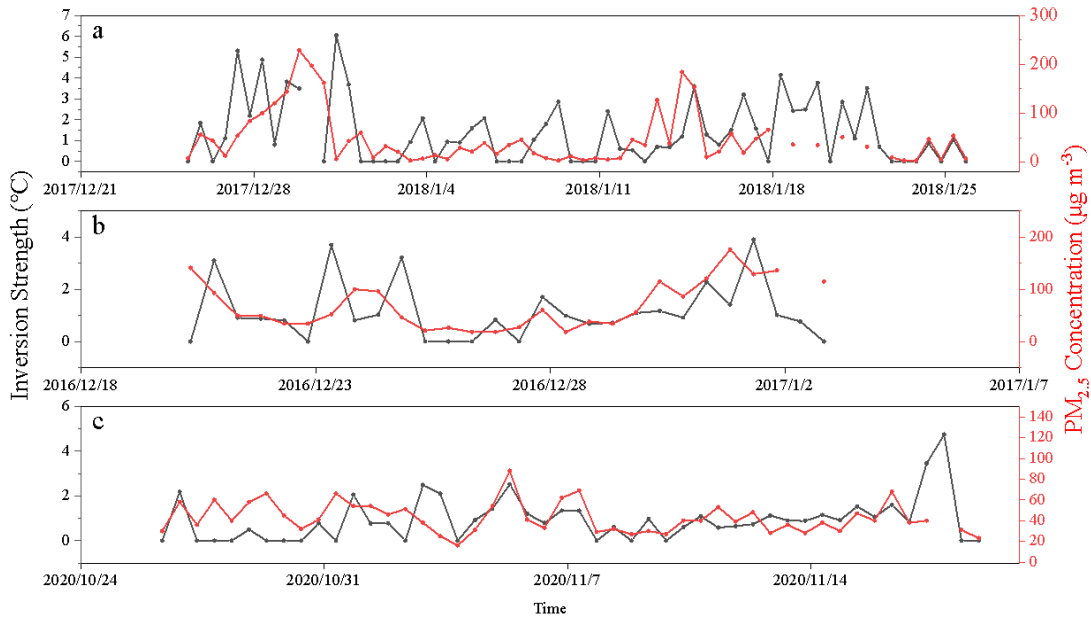


Fig. S22 Temporal variations of temperature inversion (TI) strength and surface $\text{PM}_{2.5}$ concentrations during severe pollution episodes in representative cities. (a) Beijing (BTH region), (b) Nanjing (YRD region), and (c) Yangjiang (PRD region). The black line represents TI strength (ΔT , left axis), and the red line represents $\text{PM}_{2.5}$ concentration (right axis).

5. One of the most intriguing findings is the negative correlation between EI strength and PM in southern China. The proposed explanation—a "transport-suppression mechanism" where EIs cap the boundary layer and isolate it from northerly pollutant inflow—is plausible but remains speculative. This hypothesis should be supported with more direct evidence. The authors could analyze wind direction and speed data during these EI events to show a reduction in northerly flow, or cite studies that have documented such a synoptic setup in southern China.

Response: We thank you for this insightful comment. You correctly pointed out the need to clarify the distinct pollution mechanisms in South China, particularly why inversions there seem to correlate with better air quality.

To investigate this, we combined Potential Source Contribution Function (PSCF) analysis with a detailed examination of wind fields during inversion (EI) versus non-inversion periods. The results reveal a mechanism driven by "Ventilation vs. Stagnation":

EI Periods (Fig. S24b): Our data shows that EIs in South China are synchronized with northerly winds. While the PSCF results (Fig. S23) identify Central China as a potential upstream source, the strong momentum of these northerly winds acts as a "sweeper," transporting pollutants rapidly into the South China Sea. This strong horizontal advection dominates over the vertical stability of the inversion, leading to lower PM levels.

Non-EI Periods (Fig. S24a): In contrast, non-inversion periods are dominated by weak southerly

winds. We found that the Nanling Mountains play a critical role here, not by blocking incoming pollution, but by blocking the northward dispersion of local emissions. This creates a semi-enclosed stagnation zone over the Pearl River Delta, facilitating local accumulation despite the absence of an inversion lid.

To maintain the conciseness of the main text while addressing your concern, we have added a pointer to the Supplementary Material regarding 'this phenomenon'. Detailed mechanistic evidence, including PSCF maps and wind field analysis, is now provided in Text S3 of the supplement.

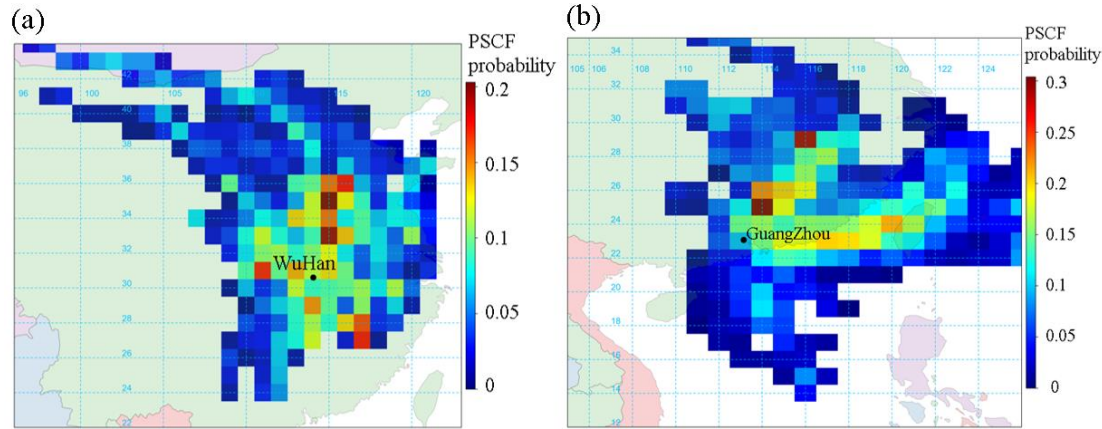


Figure S23 Spatial distribution of the Potential Source Contribution Function (PSCF) values for PM2.5 during the study period. The analysis is based on 48-h backward trajectories at an altitude of 500 m. (a) Wuhan (representative of Central China), showing dominant potential sources from the North China Plain. (b) Guangzhou (representative of South China), indicating potential transport pathways primarily from Central China and the eastern coast.

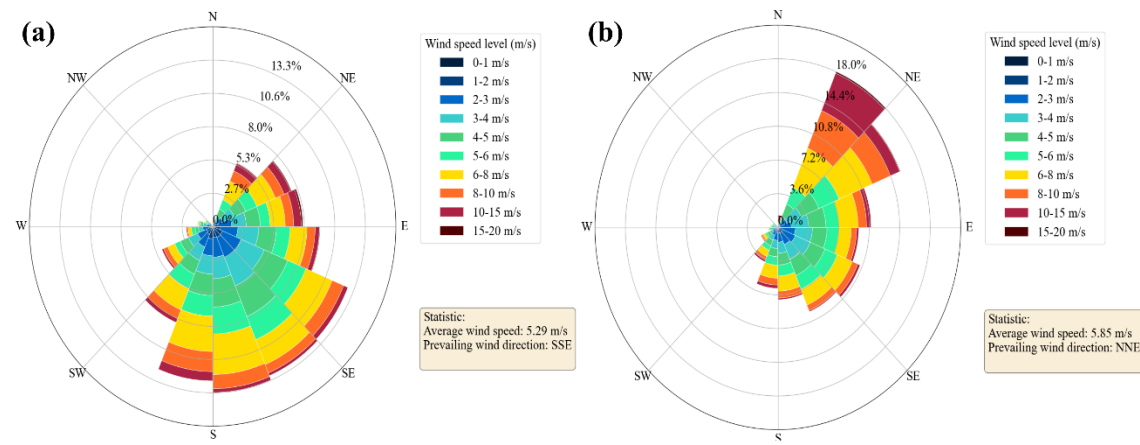
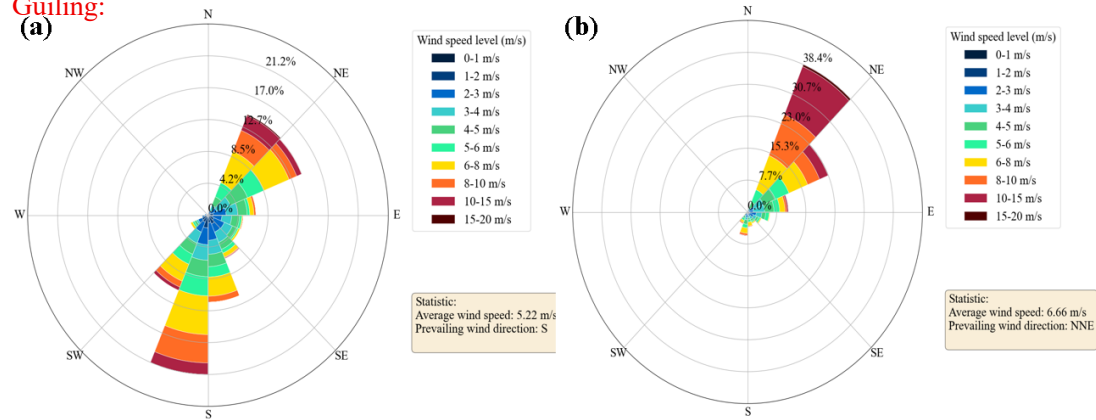


Figure S24. Roses of the mean boundary-layer wind (0–1000 m) in SC. (a) Patterns during non-inversion periods. (b) Patterns during the presence of EIs. Note that EIs are typically associated with stronger northerly winds (ventilation), while non-inversion periods are dominated by weaker southerly winds.

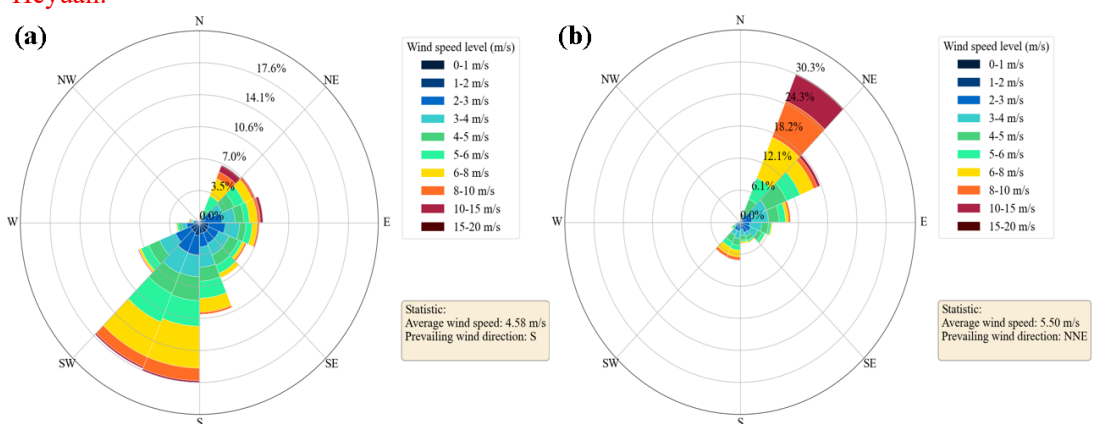
Below are the wind rose diagrams for selected cities in South China during EI and non-EI periods (for the response letter only).

(a) Patterns during non-inversion periods. (b) Patterns during the presence of EI.

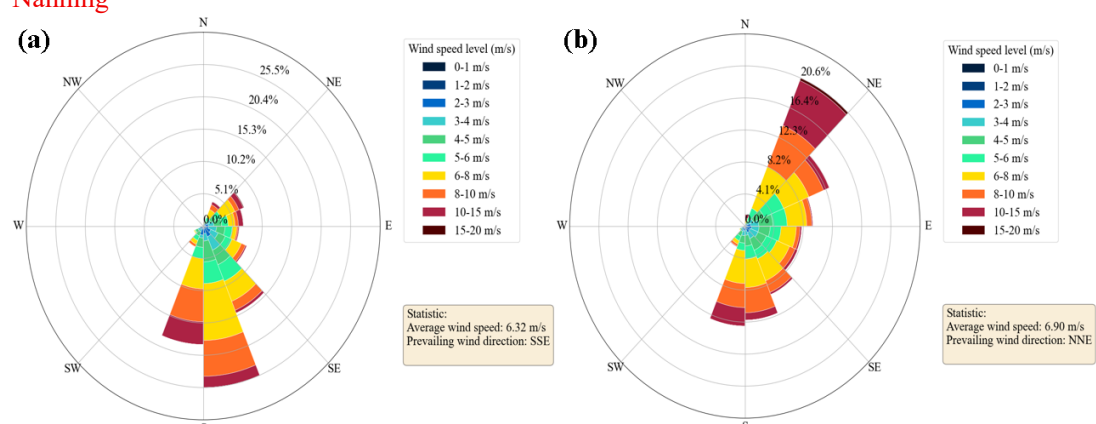
Guiling:



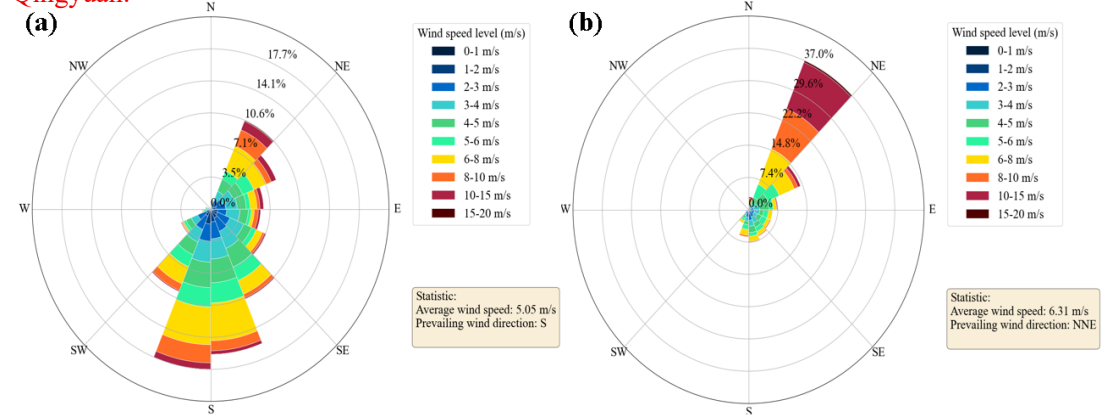
Heyuan:



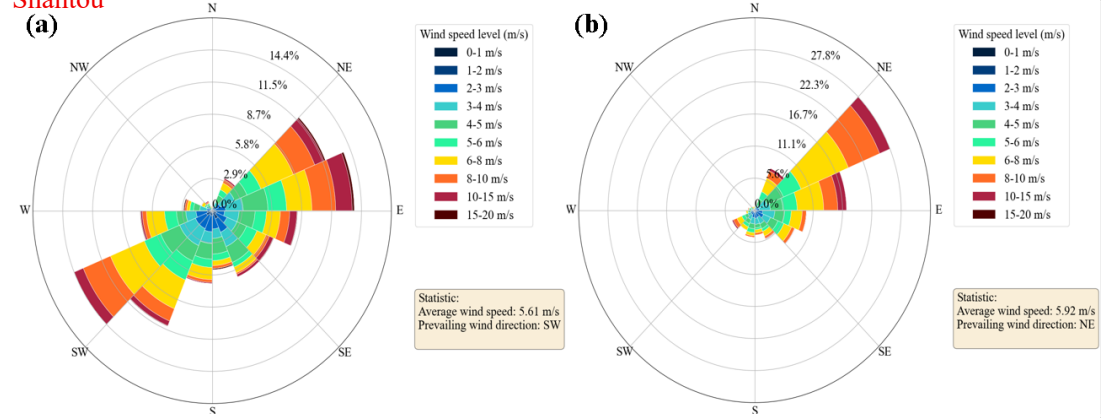
Nanning:



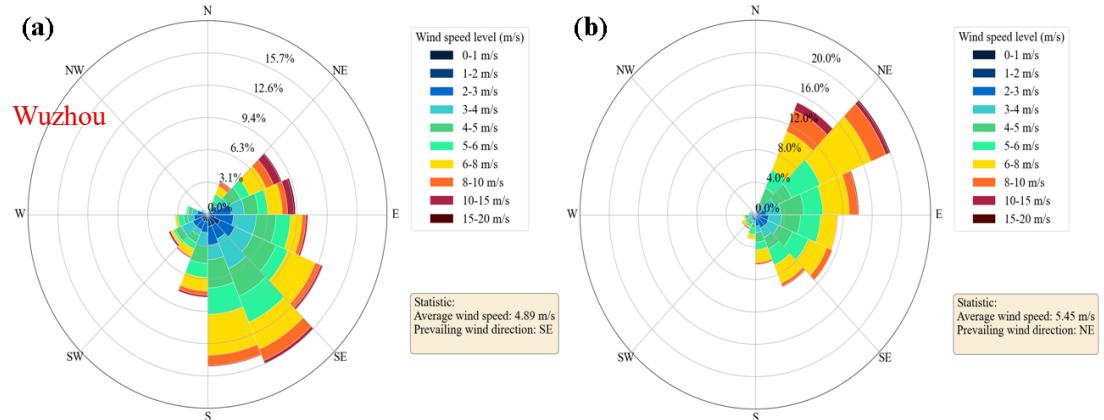
Qingyuan:



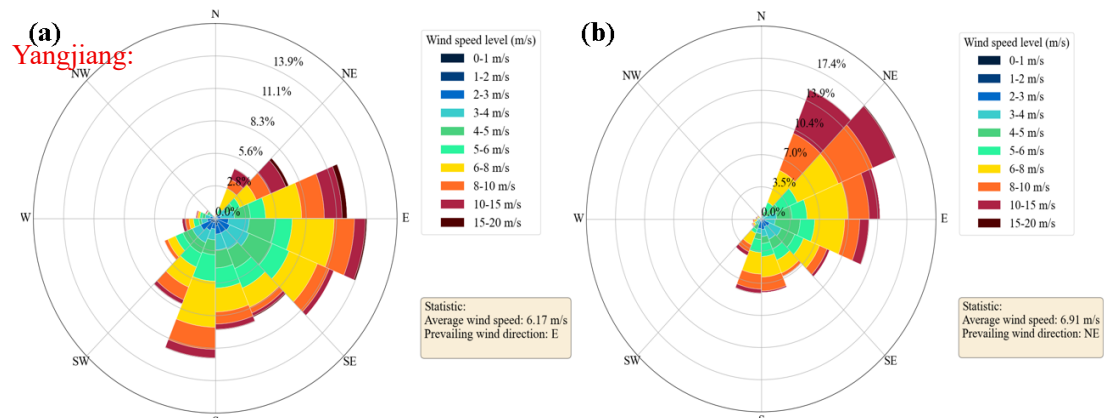
Shantou:



Wuzhou:



Yangjiang:



Specific Comments

1. Line 99-107 Does this section lack a description of Central China?

Response: Thank you very much for the suggestion. As recommended, we have added a description of Central China's geographic and climatic context in the section to better frame the study area.

The newly added section is as follows:

"Central China (CC), located in the heart of the country, experiences a transitional monsoon climate between the northern subtropical and warm temperate zones, characterized by a terrain dominated by plains and hills. Pollutants tend to accumulate in basins such as the Jianghan–Dongting Basin due to the region's enclosed topography and stable atmospheric conditions, where they further combine with polluted air masses transported from the north, resulting in regional and complex air pollution."

2. Line 211 I believe you are describing three figures rather than two. "(Fig S2, 4a)" changed to "(Fig S2, S3, and 4a)".

Response: We appreciate your careful reading. This was indeed an error in the figure citation. We have revised the sentence to correctly reference all three relevant figures: "(Fig S5, S6, and 4a)". (The supplementary materials have been updated, and the figure numbers have been modified accordingly.)

3. Figure 2: The color scheme for the different regions in the bar plot is difficult to distinguish. Please use a more distinct and colorblind-friendly palette.

Response: Thank you for your suggestion regarding the color scheme in Figure 2. We agree that the original palette may not be sufficiently distinct or color-blind-friendly.

We have improved the visual clarity of Figure 2 through the following revisions: The color contrast between regional curves has been enhanced, and uniform markers have been replaced with distinct symbols to facilitate inter-regional comparison. The originally ambiguous color representing the "Southwest" region has been adjusted to ensure clear differentiation. The vertical resolution of the histogram has been refined from 200 m to 100 m bins, allowing more explicit discrimination between the base-height distributions of surface-based inversions (SBIs) and elevated inversions (EIs).

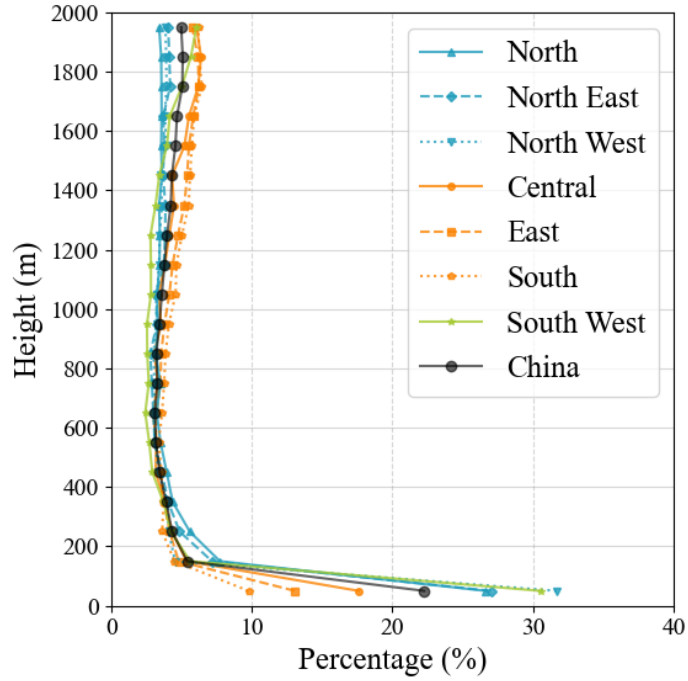


Fig.2 Vertical distribution of inversion base height: fraction of total inversions per height bin.

4. **Figure 8:** The presentation of the results in this figure is very dense. Consider breaking it down into two separate figures (e.g., one for 08:00 BJT and one for 20:00 BJT) for improved clarity.
 Response: Thank you for your constructive suggestion regarding the clarity of Figure 8. We apologize for the insufficient clarity in its original description and will revise the explanation accordingly.

In the manuscript, Figure 8 presents the seasonal average of $PM_{2.5}$ differences between inversion and non-inversion conditions, combining data from both 08:00 and 20:00 BJT. To address your concern and improve readability, we have already included time-resolved analyses in the Supplementary Material.

Both supplementary figures include significance markers from two-sample t-tests, allowing direct comparison of diurnal inversion impacts. We have revised the relevant sentence in Section 4.2.2 to clarify this point: “We quantify inversion impacts by contrasting the daily mean $PM_{2.5}$ concentrations under inversion and non-inversion conditions, with statistical significance assessed using two-sample t-tests (Fig. 8). The time-resolved analyses for 08:00 and 20:00 BJT are shown in Figs. S12 and S13.”

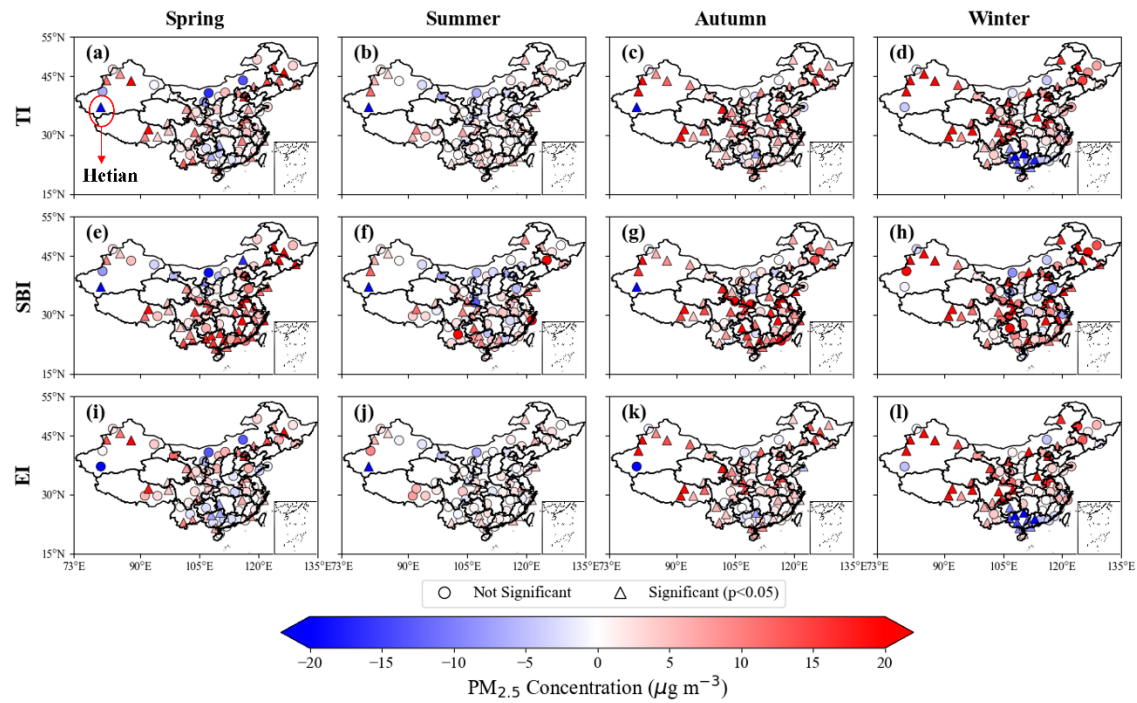


Fig S12. Distribution of PM_{2.5} concentration differences with and without temperature inversion at BJT 08:00.

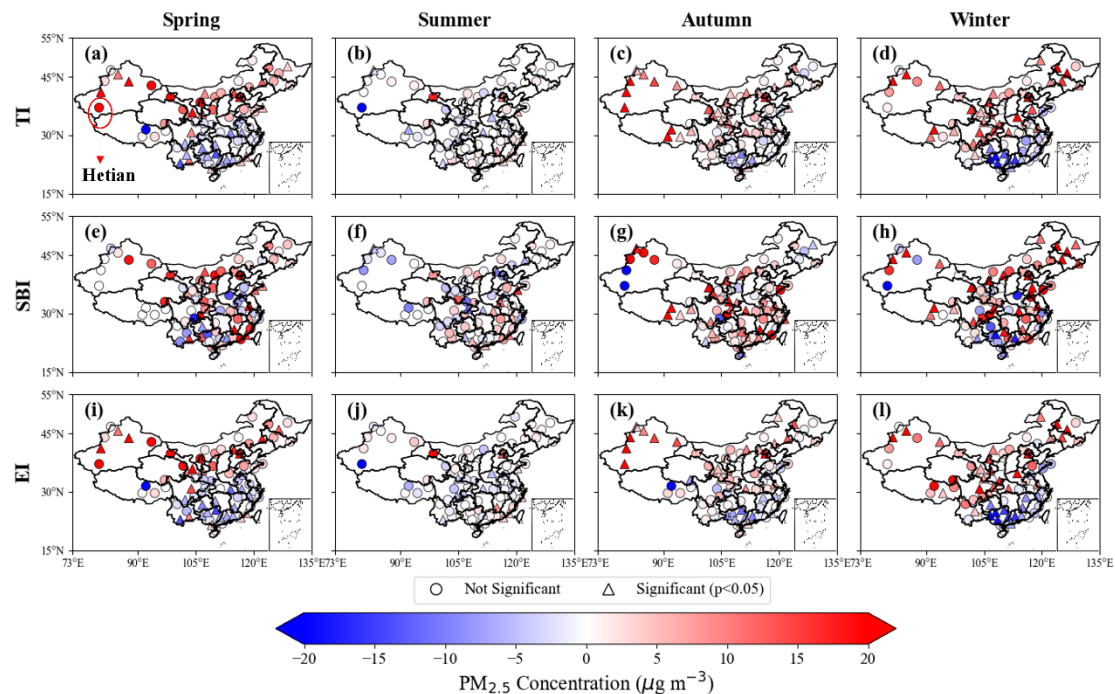


Fig S13. Distribution of PM_{2.5} concentration differences with and without temperature inversion at BJT 20:00.

5. Line 295-297: The location of 'Hetian' in southern Xinjiang, as discussed in the text, should be marked on **Figure 8** to improve readability.

Response: We thank the reviewer for this constructive suggestion. As recommended, we have marked the location of the Hetian station in southern Xinjiang on Figure. 8a in the revised manuscript.

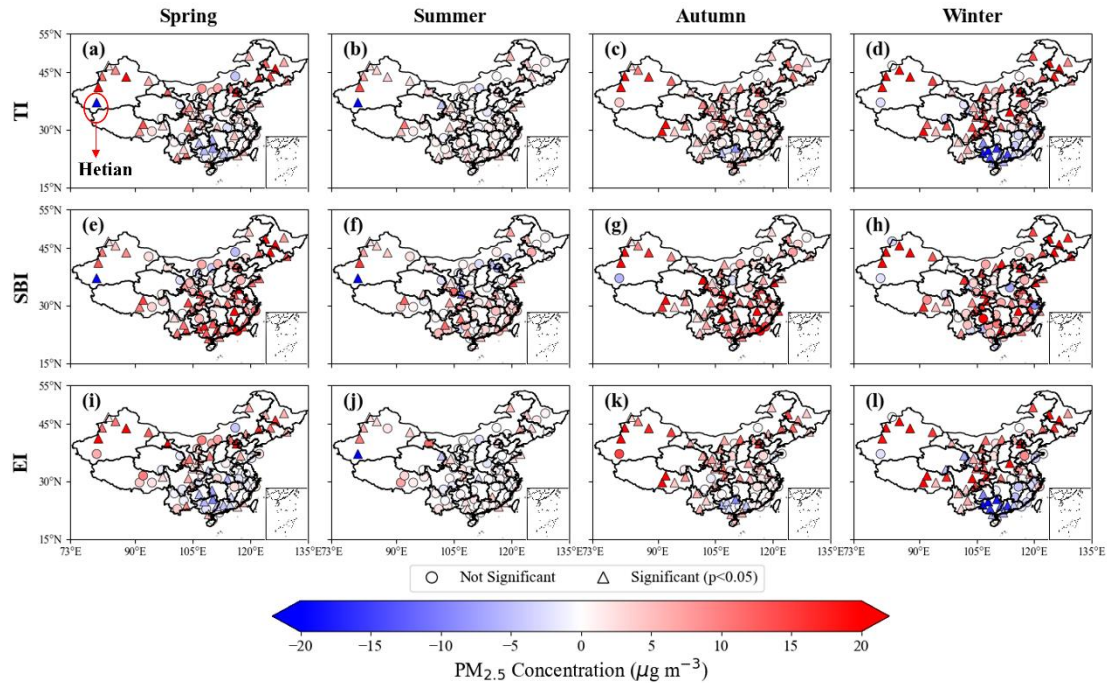


Fig.8 Distribution of PM_{2.5} concentration differences with and without temperature inversion. The larger circle indicates significance at the 95% level (*t*-test)

6. **Line 334** Extra parentheses in citation “(Liu et al., 2022)” → Remove extra parenthesis

Response: Thank you for catching this typographical error. The extra parenthesis has been removed, and the citation now correctly reads “(Liu et al., 2022)” in the revised manuscript.

7. **Line 354-356:** The statement "a deep but weak inversion can be eroded by mechanical turbulence more readily than a shallow but intense one" is a key physical insight. This point could be emphasized earlier in the manuscript to better frame why strength is a more dominant factor than thickness.

Response: Thank you very much for the suggestion. Following your suggestion, we have relocated and expanded this statement to an earlier section of the discussion (Section 4.2.2) to better frame the physical rationale behind why inversion strength is a more dominant predictor than thickness.

Revised: By contrast, inversion thickness shows a much weaker and less uniform association with PM_{2.5} (Fig. S14). SBI thickness is generally positively correlated with PM_{2.5} (except in

NEC). For EI, significant thickness-PM2.5 relationships appear only in NEC and NWC ($R^2 = 0.86$ and 0.92 , respectively); elsewhere, EI thickness exerts negligible influence. Together, these results establish inversion strength—not thickness—as the dominant predictor of PM_{2.5} accumulation (Fig. 9 vs. Fig. S14)., Thickness primarily defines the volume of the trapping layer: a deep but weak inversion can be eroded by mechanical turbulence more readily than a shallow but intense one. This mechanism ensures that a stronger temperature gradient yields greater static stability and more effective suppression of turbulent mixing (Liu et al., 2022).

8. **Language and Abbreviations:** The manuscript is generally well-written. A minor check for consistent use of abbreviations is recommended (e.g., "TI" is used throughout, but the full term is sometimes repeated unnecessarily).

Response: Thank you for your careful reading and helpful suggestion regarding abbreviation consistency. We have now systematically reviewed the entire manuscript to ensure that "temperature inversion (TI)" is defined at its first occurrence and subsequently referred to consistently as "TI." All other abbreviations have been checked for uniformity.

Reference:

Fan, Hao, Chuanfeng Zhao, and Yikun Yang. 2020. "A Comprehensive Analysis of the Spatio-Temporal Variation of Urban Air Pollution in China during 2014–2018." *Atmospheric Environment* 220: 117066. <https://doi.org/10.1016/j.atmosenv.2019.117066>.

Guo, Jianping, Xinyan Chen, Tianning Su, et al. 2020. "The Climatology of Lower Tropospheric Temperature Inversions in China from Radiosonde Measurements: Roles of Black Carbon, Local Meteorology, and Large-Scale Subsidence." *Journal of Climate* 33 (21): 9327–50. <https://doi.org/10.1175/JCLI-D-19-0278.1>.

Huang, Qianqian, Yiqi Chu, and Qianhui Li. 2021. "Climatology of Low-Level Temperature Inversions over China Based on High-Resolution Radiosonde Measurements." *Theoretical and Applied Climatology* 144 (1–2): 415–29. <https://doi.org/10.1007/s00704-021-03536-w>.

Kahl, Jonathan D. 1990. "Characteristics of the Low-level Temperature Inversion along the Alaskan Arctic Coast." *International Journal of Climatology* 10 (5): 537–48. <https://doi.org/10.1002/joc.3370100509>.

Sun, Zhixu, Jiani Tan, Fangting Wang, et al. 2024. "Regional Background Ozone Estimation for China through Data Fusion of Observation and Simulation." *Science of The Total Environment* 912 (February): 169411. <https://doi.org/10.1016/j.scitotenv.2023.169411>.